Available online at www.sciencedirect.com

ScienceDirect

Procedia Engineering 64 (2013) 1495 – 1504

Procedia Engineering

www.elsevier.com/locate/procedia

International Conference On DESIGN AND MANUFACTURING, IConDM 2013

Experimental Determination of Machining Responses in Machining Austempered Ductile Iron (ADI)

Kumar K.M.[a,*], Hariharan P[b]

[a]*Department of Mechanical Engineering,St.Joseph's College of Engineering,Chennai – 600 119, India.*
[b]*Department of Manufacturing Engineering,College of Engineering Guindy,Chennai – 600 025, India*

Abstract

This work investigates the machining characteristics of Austempered Ductile Iron (ADI) using Electrical Discharge Machining (EDM) process with copper as an electrode. Experiments have been carried out to analyze the effect of each parameter on the machining characteristics, and to predict the optimal choice for each EDM parameters such as peak current, pulse on time, pulse off time and tool geometry. Three different specimens were austenised at 900° C for 90 min and then austempered in a salt bath at 360° C, 380° C, and 400° C for 120 min. Experiments have been designed as per Taguchi's L_{18} orthogonal array. Analysis of variance (ANOVA) is used to find the level of significance of machining parameters. Machining responses such as the metal removal rate (MRR), Tool wear rate (TWR), surface roughness (SR) and taper angle (DVEE) for entrance – exit of the tool was studied while machining the Austempered Ductile Iron (ADI) with copper as an electrode. Discharge current, Pulse on time and Austempering temperature are found most influential parameters on each performance measure. Tool geometry is found the least influential parameters.

Selection and peer-review under responsibility of the organizing and review committee of IConDM 2013

Keywords: Austempered ductile iron (ADI); EDM; Taguchi's; ANOVA; L_{18} array.

1. Introduction

Austempered ductile iron (ADI) was studied thoroughly in the late 1970s. ADI offers excellent characteristics of strength, ductility and toughness. It is also provides excellent fatigue strength and wear resistance [1-6]. ADI is better than forged aluminium with respect to weight to strength ratio. As an ADI contains graphite, its impact and

* Corresponding author. Tel.: +91-044-245-00594; fax: +91-044-245-00861.
*E-mail address:*kumar_tjit@yahoo.com

Selection and peer-review under responsibility of the organizing and review committee of IConDM 2013
doi:10.1016/j.proeng.2013.09.231

tensile strength is better than those of steel [7]. Higher strength and hardness of ADI have caused many researchers and engineers to doubt the machinability of this material (8).As a result, non-traditional machining techniques such as electro-discharge machining must be employed (6). Since the ADI is a newer material, its machinability has not been studied using non-traditional machining except the work done by Che Chung Wang et al [6], Kataoka et al [9], who used laser machining and Chow et al (10), who used modified traditional machining technique.

Electrical Discharge Machining (EDM) was first introduced in the 1940's as a crude device used to cut broken machining tools from expensive in-process parts. In electrical discharge machining, it is important to select machining parameters for achieving optimal machining performance. The Taguchi method has become a powerful tool in the design of experiment methods [11] for engineering optimization of a process. The S/N ratio characteristics can be divided into two categories when the characteristic is continuous:

Smaller the better characteristics:

$$S/N = -10\ log\frac{1}{n}\ (\sum y^2) \quad (1)$$

Larger the better characteristics:

$$S/N = -10\ log\frac{1}{n}\ \left(\sum \frac{1}{y^2}\right) \quad (2)$$

Where y is the average of observed data, n the number of observations. Analysis of Variance (ANOVA) is used to determine the design parameters or their interactions significantly influencing the response. It is possible to assess quantitatively the influence of EDM parameters on SR, MRR and TWR through derivation of some empirical equations. Extensive research has been carried out in the field of EDM and paper have been published investigating the influence of EDM parameters over machining responses of different work piece material and tool electrode combinations [12-14], however, very little published work is available corresponding to Austempered ductile iron and copper tool combination with different tool geometries as per a published literature survey. Thus, efforts have been made to investigate the EDM characteristics of ADI by DOE techniques in this work.

Nomenclature

A	ampere
V	voltage
ρ_w	density of work piece material
ρ_e	density of tool material
T	time

2. Experiment Details

In the present investigation, the experiments were performed on ELECTRONICA PSR 35 EDM machine. EDM oil is used as a dielectric fluid. Its parts are described in the table 1. A power supply unit of the EDM machine shown in table 2.

2.1. Work Piece Material

The material employed in this study is Austempered ductile Iron (ADI). Specimens were prepared under different austenizing temperature and austempering temperatures. Three different specimens were austenised at 900° C for 120 min and then austempered in a salt bath at 360° C, 380° C, and 400° C for 90 min. The final dimensions of the

work piece are 100 x 50 x 3 mm. Its density is 7.22g cm^{-3}. The chemical composition of Austempered Ductile Iron is shown in the table 3.

2.2. The Cutting Tool

The copper electrode is with a density of 8.79g/cc.. Few of the properties of commercial electrolytic copper are tabulated below (table 5). In this experiment, the copper is machined into three geometric shapes, each having one similar geometrical dimension-at least one side of 8 mm. It is machined into circular, square and triangular shapes are shown in fig. 1. The dimensions for each of the copper tools are as follows: Square: Side = 8mm, Triangle: Side = 8mm, Circle: Diameter = 8mm.

Fig. 1. Square, triangle and circle shaped copper electrode.

Table 1. Specifications of the EDM machine.

MODELS	UNIT	S 35 – 5030
Work Tank Dimensions	mm	750 x 450 x 400
Table Size	mm	500 x 300
X - Axis Travel - With Ball Screw.	mm	280
Y - Axis Travel - With Ball Screw.	mm	200
Z - Axis Travel - With Ball Screw.	mm	250

Table 2. Specifications of power supply.

PARAMETER	UNITS	EMS 5030
Maximum Current	A	40
Maximum Open Circuit Voltage	V	75-80
Material Removal Rate	mm^3min^{-1}	150
Pulse-on time	Ms	99
Pulse-off time	Ms	9

Table 3. Chemical composition of Austempered Ductile Iron.

Composition	C	Mn	Si	S	P	Cr	Cu	Mg
In %	3.66	0.21	2.76	0.021	0.011	0.03	0.28	0.04

Table 4. Mechanical properties.

S.NO	PROPERTIES	RESULT
1	Tensile Strength	440.94n/mm^2
2	Yield Stress	392.58n/mm^2
3	Elongation	4.60%

The parameters chosen based on a literature survey and preliminary investigations. In total five parameters were considered, among that there are three electrical parameters including pulse current, pulse on time and pulse off time, and fourth one is tool geometry along with fifth parameter is austempering temperature. In the present

investigation Taguchi's orthogonal array L_{18} was selected and it has 18 rows and 8 columns. The analysis of the experimental data was carried out MINITAB 16 software. Table 6 shows the details of the parameters and its level values. Table 7 shows the L_{18} orthogonal array and experimental data. New copper tool electrode was used in every experiment. Figure 2 shows the completed work piece.

Table 5. Properties of electrode.

Properties	Electrolytic
Copper, %	99-99.5
Weight Loss in H_2, %	0.1-0.75
Acid Insoluble, %	0.03 max
Density, g/cm^3	8.79

Table 6. EDM process parameters and levels.

PARAMETERS	LEVELS		
	L1	L2	L3
Current (A)	10	15	20
Pulse on-time (μs)	35	55	75
Pulse off-time (μs)	7	8	9
Tool electrode geometry	Square	Triangle	Circle
Austempering Temperature(°C)	360°	380°	400°

In the present investigation, the Material Removal Rate in mm^3 is used to evaluate the machining parameter. The MRR is expressed as:

$$MRR = WRW / (\rho_w \, x \, T) \quad (3)$$

Where WRW is the Work piece Removal Weight in grams, ρ_w is the density of the work piece in g/mm^3 and T is the machining time in minutes. Similarly the Electrode Wear Rate in mm^3 is used to evaluate the machining parameter. The EWR is expressed as:

$$EWR = EWW / (\rho_e \, x \, T) \quad (4)$$

Where EWW is the Electrode Wear Weight in grams, ρ_e is the density of the tool in g/mm^3 and T is the machining time in minutes. Surface roughness is measured using a surface roughness gauge. The surface roughness gauge used is 'MAHRSURF PS 1' as shown in the Figure 3. The deviation between entrance and exit (DVEE), otherwise known as taper is measured using a Co-ordinate Measuring Machine (CMM). The taper is observed in degrees.

3. Analysis of Experimental results

3.1. Factor effect on Material Removal Rate (MRR)

Table 8 shows the experimental results of MRR and its corresponding S/N ratio, whose ANOVA results are shown in table 9. ANOVA table for MRR indicates that tool geometry is the most dominant factor having percentage contribution as 80.9, followed by pulse off time and current. This is due to higher discharge current more spark energy is induced and remove the more materials. The MRR and pulse on time which indicates that initially MRR increases with increase in pulse on time but after certain time MRR decreases with further increase in pulse on

time. This may be due to, until the most favorable value pulse on time increases the power concentration of the discharge energy and further than that it reduces the power concentration [20]

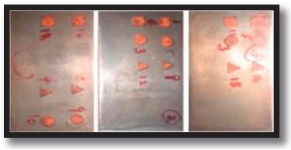

Fig. 2. The machined work piece.

Fig. 3. Surface roughness gauge.

Table 7: L_{18} Orthogonal Array and experimental data.

Exp No	Parameters				
	Current (A)	Pulse on time(µs)	Pulse off time (µs)	Tool Electrode Geometry	Austempering temperature(ºC)
1	10	35	7	Square	360
2	10	55	8	Triangle	380
3	10	75	9	Circle	400
4	15	35	7	Triangle	380
5	15	55	8	Circle	400
6	15	75	9	Square	360
7	20	35	8	Square	400
8	20	55	9	Triangle	360
9	20	75	7	Circle	380
10	10	35	9	Circle	380
11	10	55	7	Square	400
12	10	75	8	Triangle	360
13	15	35	8	Circle	360
14	15	55	9	Square	380
15	15	75	7	Triangle	400
16	20	35	9	Triangle	400
17	20	55	7	Circle	360º
18	20	75	8	Square	380º

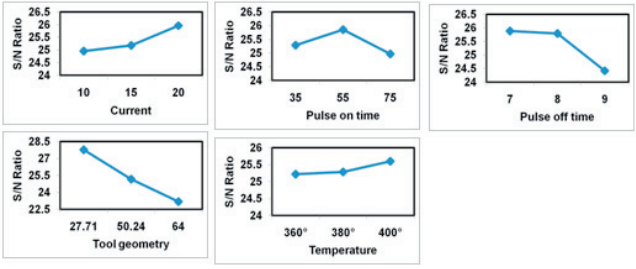

Fig. 4.Main effect plot for S/N Ratio – MRR.

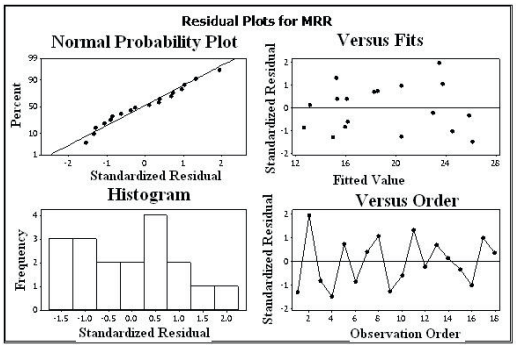

Fig.5. Residual plots for Material Removal Rate (MRR).

Table 8. Experimental results.

Exp No	MRR (mm3/min)	S/N Ratio(dB)	TWR (mm3/min)	S/N Ratio(dB)	SR (μm)	S/N Ratio(dB)	DVEE (°)	S/N Ratio(dB)
1	13.73	22.75	0.19	14.63	5.84	-15.33	0.57	4.88
2	25.54	28.14	0.14	17.09	5.99	-15.55	0.80	1.94
3	15.10	23.58	0.09	21.35	7.03	-16.94	0.45	6.94
5	24.61	27.82	0.13	17.97	6.11	-15.72	0.77	2.27
6	19.37	25.74	0.10	20.40	6.97	-16.86	0.55	5.19
7	11.73	21.39	0.16	15.69	5.99	-15.55	0.52	5.68
8	16.38	24.29	0.10	20.39	6.97	-16.86	0.47	6.56
9	24.75	27.87	0.17	15.56	5.24	-14.39	0.78	2.16
10	19.17	25.65	0.12	18.39	6.32	-16.01	0.70	3.10
11	15.50	23.80	0.11	19.24	6.30	-15.99	0.49	6.20
12	16.47	24.33	0.11	19.23	7.45	-17.44	0.50	6.02
13	22.72	27.13	0.18	14.75	5.92	-15.45	0.87	1.21
14	19.00	25.58	0.17	15.41	5.79	-15.25	0.65	3.74
15	13.21	22.42	0.10	19.80	6.55	-16.32	0.51	5.85
16	25.56	28.15	0.10	20.43	6.98	-16.88	0.75	2.50
17	23.65	27.48	0.08	21.72	6.35	-16.06	0.70	3.10
18	21.41	26.61	0.16	15.93	5.63	-15.01	0.72	2.85

Table 9. ANOVA table for MRR.

FACTORS	DOF	SS	MS	F	P	% OF CONTRIBUTION
CURRENT	2	3.344	1.672	16.831	0.014	4.26
PULSE ON TIME	2	2.435	1.217	12.255	0.492	3.10
PULSE OFF TIME	2	8.056	4.028	40.548	0.002	10.25
TOOL GEOMETRY	2	63.565	31.783	319.933	0.000	80.90
TEMPERATURE	2	0.476	0.238	2.397	0.460	0.61
ERROR	7	0.695	0.099			0.89
TOTAL	17	78.572				100

During the pulse off time no energy is applied to the work piece surface and results in low MRR. Then again, since the time available for the application of heat energy on the work piece surface, the top surface temperature of the work piece increases as the pulse off time decreases. The same observations are reported by the previous researchers. [17-19]. Tool geometry does not have considerable effect on MRR.

3.2. Factor effect on Tool Wear Rate (TWR)

Experimental results of TWR and its corresponding S/N ratio are represented in table 8. The table 10, ANOVA result for TWR shows that Austempering temperature is the most dominant factor having the percentage of contribution as 89.3, followed by pulse off time and current. Here, Fig 6. Shows that TWR increases as discharge current, pulse of time and Austempering temperature increases. High discharge current induces high spark energy which removes the more material from the work piece and tool electrode. TWR increases as increasing the Austempering temperature of the work materials.TWR increases initially with increment in tool geometry cross

section but decreases with further increase in tool geometry cross section. TWR verses pulse on time shows that initially TWR decreases with increasing pulse on time but after certain time TWR increases with increasing the pulse on time. This is due to higher pulse on time i.e. duration time and discharge current indicates that more spark energy for a longer time which results in larger removal of tool electrode.

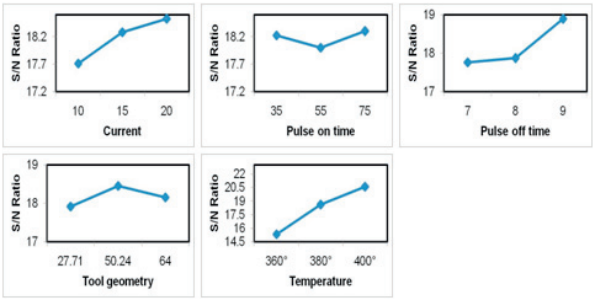

Fig 6.Main Effect Plot for S/N Ratio – TWR

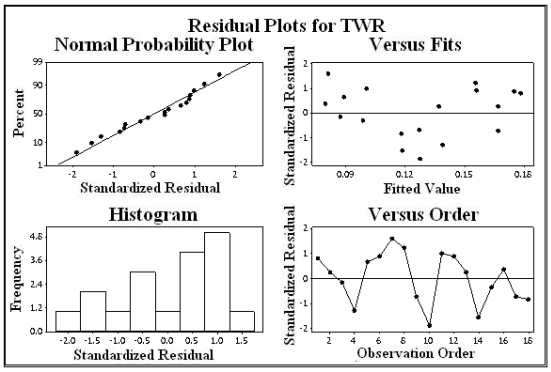

Fig.7. Residual plots for Tool Wear Rate (TWR).

3.3. Factor effect on Surface Roughness (SR)

Experimental results of Surface roughness (SR) and their corresponding S/N ratio are shown in table 8. ANOVA results for SR reported in table 11, shows that Austempering temperature is the most dominant factor having the percentage of contribution as 78.25, followed by tool geometry and current. Fig 8. shows that SR increases when the discharge current and pulse off time increases, whereas the pulse on time at higher values reduces the SR.

Table 10. ANOVA table for TWR.

FACTORS	DOF	SS	MS	F	P	% OF CONTRIBUTION
CURRENT	2	2.104	1.052	3.359	0.073	2.22
PULSE ON TIME	2	0.292	0.146	0.466	0.798	0.31
PULSE OFF TIME	2	4.668	2.334	7.452	0.051	4.92
TOOL GEOMETRY	2	0.855	0.427	1.364	0.432	0.90
TEMPERATURE	2	84.689	42.344	135.196	0.000	89.33
ERROR	7	2.192	0.313			2.31
TOTAL	17	94.799				100

Table 11. ANOVA table for SR.

FACTORS	DOF	SS	MS	F	P	% OF CONTRIBUTION
CURRENT	2	0.456	0.228	6.641	0.007	4.22
PULSE ON TIME	2	0.339	0.169	4.929	0.010	3.14
PULSE OFF TIME	2	0.133	0.066	1.931	0.082	1.23
TOOL GEOMETRY	2	1.180	0.590	17.176	0.000	10.93
TEMPERATURE	2	8.453	4.227	123.005	0.000	78.26
ERROR	7	0.241	0.034			2.23
TOTAL	17	10.802				100

It was observed that when a pulse on time increased, the machined work piece surface had a higher surface roughness due to irregular topography. This is due to machined surface consists of a huge amount of overlapping craters that are formed by spark discharges. The size of these craters depends on the discharge energy and duration. More is the discharge energy; the largest are the craters resulting in more SR. The tool geometry and Austempering temperature have an inverse relationship with the SR.

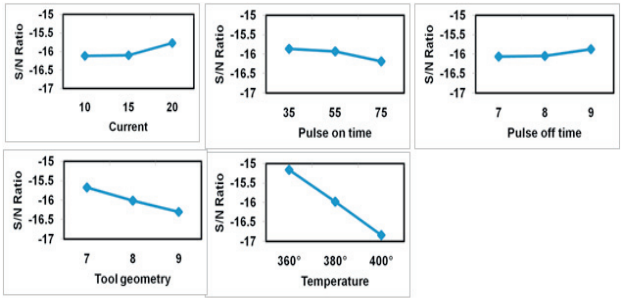

Fig. 8. Main effect plot for S/N Ratio – SR.

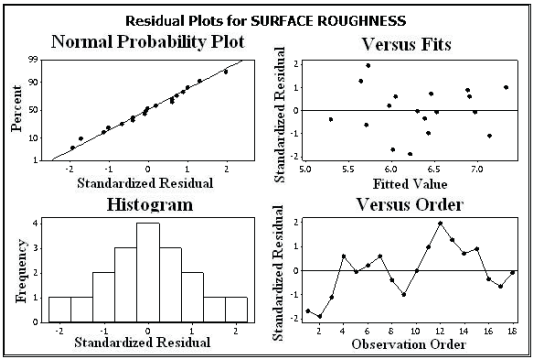

Fig.9. Residual plots for Surface roughness (SR).

3.4. Factor effect on Deviation of Entrance and Exit angle (DVEE)

Experimental results of deviation of entrance and exit (DVEE) and their corresponding S/N ratio are shown in table 8. ANOVA result for DVEE, table 12 reported that tool geometry is the most dominant factor having the percentage of contribution as 67.22, followed by Austempring temperature and pulse off time.As shown in Fig 10. DVEE is more when increase the pulse off time, tool geometry and Austempering temperature. A cross section of the tool geometry plays an important role to increase or decrease the DVEE. The cross sectional area of the tool electrode is more, lesser the DVEE as in the result. The initial value of the current and pulse on time was increasing the DVEE, further more increasing these two factors the deviation of entrance and exit value decreasing.

Four residual plots (Fig.5, 7, 9, 11) are drawn for estimating the accuracy of the model. The histogram plot indicates a mild tendency for the non normality; however the normal probability plots of these residuals do not reveal any abnormality. Residual versus fitted value and residual versus observation order plot do not indicate any undesirable effect.

Table 12: ANOVA table for DVEE

FACTORS	DOF	SS	MS	F	P	% OF CONTRIBUTION
CURRENT	2	1.725	0.862	3.753	0.057	3.06
PULSE ON TIME	2	0.752	0.376	1.636	0.115	1.33
PULSE OFF TIME	2	6.292	3.146	13.692	0.001	11.15
TOOL GEOMETRY	2	37.950	18.975	82.580	0.000	67.23
TEMPERATURE	2	8.124	4.062	17.677	0.000	14.39
ERROR	7	1.608	0.230			2.85
TOTAL	17	56.451				100

4. Regression Equations

The following regression equations were found using the least-square method in Minitab-R16 software. In this equation, following units are used to represent the parameters, current in ampere, pulse on time in microseconds, pulse off time in microsecond, tool geometry in square millimeter and Austempering temperature in degree Celsius.

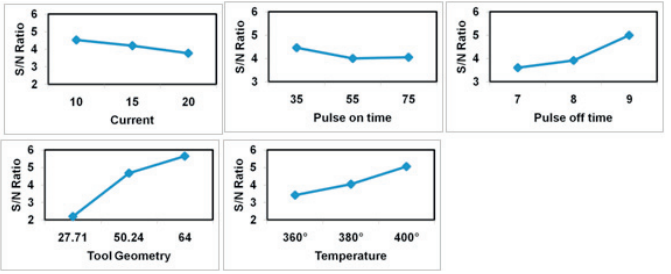

Fig. 10. Main effect plot for S/N ratio – DVEE.

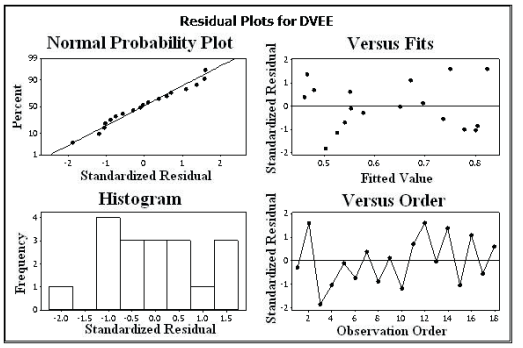

Fig.11. Residual plots for DVEE.

The regression equation is

$$MRR = 36.1 + 0.199\ CURRENT - 0.0123\ PULSE\ ON\ TIME - 1.42\ PULSE\ OFF\ TIME - 0.274\ TOOL\ GEOMETRY + 0.0133\ TEMPERATURE \quad (5)$$

$$R\text{-}Sq = 95.2\%\quad R\text{-}Sq\ (adj) = 93.1\%$$

The regression equation is

$$TWR = 0.952 - 0.00130\ CURRENT - 0.000043\ PULSE\ ON\ TIME - 0.00720\ PULSE\ OFF\ TIME - 0.000147\ TOOL\ GEOMETRY - 0.00194\ TEMPERATURE \quad (6)$$

$$R\text{-}Sq = 92.4\%\quad R\text{-}Sq\ (adj) = 89.3\%$$

The regression equation is

$$SURFACE\ ROUGHNESS = -5.24 - 0.0250\ CURRENT + 0.00583\ PULSE\ ON\ TIME - 0.0725\ PULSE\ OFF\ TIME + 0.0124\ TOOL\ GEOMETRY + 0.0306\ TEMPERATURE \quad (7)$$

$$R\text{-}Sq = 96.3\%\quad R\text{-}Sq\ (adj) = 94.8\%$$

The regression equation is

$$DVEE = 2.32 + 0.00433\ CURRENT + 0.000875\ PULSE\ ON\ TIME - 0.0467\ PULSE\ OFF\ TIME - 0.00714\ TOOL\ GEOMETRY - 0.00287\ TEMPERATURE \quad (8)$$

R-Sq = 94.9% R-Sq (adj) = 92.7%

Their R^2 values and adjusted R^2 values confirm the validity of the model as their values are above 90% for all the responses.

6. Conclusions

This experiment was conducted to find the influence of the peak current, pulse on time, pulse off time, tool geometry and austempering temperature on the EDM performance characteristics of ADI material with copper electrode. It was also tried to formulate a mathematical model for the responses such as MRR, TWR, Surface Roughness (SR) and taper angle (DVEE). The conclusions from the analysis of these experimental results can be specified as follows:

1. Based on the experimental values, the current and pulse off time are the most significant and critical process parameters that affect all the responses, except MRR and DVEE.
2. The MRR and TWR increases with increasing current and pulse on time, but the surface roughness and DVEE inversely affect by increasing these two parameters.
3. Tool geometry does not have any reasonable influences in all the responses. However the DVEE increasing with increase the tool cross section area.
4. Austempering temperature influences only in surface roughness of the material. It was found that inversely proportionate with surface roughness.

Reference

[1] Hitchcox, AL., 1986. ADI has what it takes for high-performance gearing. Met. Prog; 130 (2) 49-51.
[2] Mohammed Seyed., Ali Boutorabi.,1993. Microstructures of austempered spheroidal graphite aluminium cast iron. Trains. Jpn Foundrym. Soc*;* 12 .14-17.
[3] Liu Qifu., 1993. Mechanism of spheroidal graphite formation in cast irons. Trans.Jpn Foundrym.Soc;12 18-24.
[4] Bing-Qing Wei., Ji Liang., 1993. Wear-resistant bainite ductile iron and its strengthening mechanism. Trans. Jpn Foundrym.Soc;12.62-68.
[5] Chang, CH., Shih TS., 1994. Ausferrite transformation in austempered alloyed ductile irons.Trans.Jpn.Foundrym.Soc;13 56-63.
[6] Wang, CC et al., 1999. Cutting austempered ductile iron using an EDM sinker. Journal of Mat. Proc. Tech; 88. 83-89.
[7] Dubensky, WJ., Rundman KB.,1985. An electron microscope study of carbide formation in ADI.AFS Trans; 64-85,385-394.
[8] Seah, KHW., Sharma SC., 1995. Machinability of alloyed Austempered ductile iron. Int. J. Mech. tools manufacturing; Vol 35 No.10, pp 1475-1479.
[9] Kataoka, Y., Miyazaki T., 1993. Laser cutting of spheroidal graphite cast iron. Trans.Jpn.Foundrym.Soc;12 37-44.
[10] Chow, HM., Chang, MJ., Wang TJ., 1996. “Cutting properties of austempered ductile iron”. Conf.of Chinese fro casting, Taipei; pp. 1-3.
[11] Lin, JL., Wang, KS., Yan, BH., Tarng, YS., 2000. Optimization of the electrical discharge machining process based on the Taguchi method with fuzzy logics. Journal of Material Processing and Technology,; Vol. 102, pp 48-55.
[12] Armendia, M., Garay, A., Iriarte LM, et al., 2010. Comparison of the machinability of Ti_6Al_4V and TIMETAL @ 54M using uncoated WC-Co tools. J Mater Proc Technol; 210: 197-203.
[13] Belgassim, O., Abusaada A., 2012. Investigation of the influence of EDM parameters on the overcut for AISI D3 tool steel. Proc IMechE, Part B: J Engineering Manufacture; 226:365-370.
[14] Belgassim, O., Abusaada A., 2012. Investigation of the influence of EDM parameters on the machined surface hardness of AISI D3 tool steel. J Eng Res; 16:31-38.
[15] Pradhan, MK., Biswas CK., 2008. “Modelling of machining parameters for MRR in EDM using response surface methodology”. Nat. Conf. on mechanism science and tech, from theory to application. NIT, Hamipur; 13-14.
[16] Kao, JY., Tarng YS., 1997. A neural network approach for the online monitoring of the electrical discharge machining process. J. Mater. Process. Technology; Vol.69, 112-116.
[17] Hansai, HK., Singh ,S and Kumar P., 2008. Numerical simulation of power mixed electric discharge machining (PMEDM) using finite element method. Math. Comp. Model; Vol 47, PP1217-1237.
[18] Saravanan paramasivam et al., 2012. Effects of electrical parameters, its interaction and tool geometry in electrical discharge machining of titanium grade 5 alloy with graphite tool. Proc IMechE Part B: J Engineering Manufacture; 1-13.